Available online at www.sciencedirect.com

SciVerse ScienceDirect

Procedia Earth and Planetary Science 5 (2012) 254 – 261

Procedia Earth and Planetary Science

2012 International Conference on Structural Computation and Geotechnical Mechanics

Dynamic Behavior Analysis of Perforated Crack Propagation in Two-Hole Blasting

Yang Renshu[a,b], Wang Yanbing[a], Xue Huajun[a], Wang Maoyuan[a], a*

[a] *School of Mechanics and Architecture Engineering , China University of Mining and Technology (Beijing), Beijing 100083 China*
[b]*State Key Laboratory for Geomechanics and Deep Underground Engineering, Beijing 100083 China*

Abstract

Using dynamic caustics blast loading system, the paper studied the dynamic behavior of perforated crack propagation on the condition of different grooving with two borehole blasting and simultaneous initiation. Two kinds of grooving modes were designed: (a) and (b). (a): A-hole double grooving, B-hole single grooving. (b): A-hole double grooving, B-hole no grooving. As can be seen from the result, stress intensity factor decreased rapidly from the maximum, oscillated, and up to the second peak, then decreased until crack arrested. K_I was almost greater than K_{II}. The velocity and acceleration showed a type of fluctuation changes as wave. Acceleration firstly came to the peak, then the velocity came to the peak again, and the process repeated many times. The energy release rate decreased rapidly, oscillated, and then decreased. It remained the same with the variation of the stress intensity factor. Dynamic energy release rate and the dynamic stress intensity factor had the same sense of dynamic fracture mechanics.

Keywords: two borehole blasting; perforated crack; crack propagation; dynamic caustics; dynamic behavior

1. Introduction

From technical effect, the requirements of rapid roadway blasting excavation can be divided into two categories: 1. break the rock into suitable fragment, easy for shipment; 2. no obvious damage in roadway surrounding rock, form well. Therefore periphery hole is caused widespread concern. Geotechnical engineering practice shows that periphery holes play a significant role in forming quality of roadway. Many scholars have studied the mechanism of perforated crack propagation in two-hole blasting [1-3].

* Corresponding author. Wang Yanbing. Tel.: 15901014167.
E-mail address: ceowyb818@163.com.

 doi:10.1016/j.proeps.2012.01.044

However, due to the complexity of the blast load, the dynamic behavior of perforated crack propagation needs further study. At macro point, dynamic behavior of crack propagation can be shown as follows: the crack length, propagation velocity, acceleration, propagation direction, dynamic stress intensity factor and dynamic energy release rate. Studying the dynamic behavior of perforated crack propagation in two-hole blasting has great significance for the guidance of engineering practice.

Caustics provide an effective experimental method for dynamic fracture mechanics study [4-7]. Measuring accuracy is high. Equipment is simple. More importantly, just through measuring the diameter of the speckle-focus, information of crack tip stress intensity can be determined. In this paper, using dynamic caustics blast load test system [8], it studied dynamic behavior of perforated crack propagation in two-hole blasting with different grooving modes.

2. Basic principle

2.1. Determination of dynamic stress intensity factors

Transmissive dynamic caustics experimental method [8]is used. The stress intensity factor of composite crack tip under dynamic loading can be shown as:

$$K_{\mathrm{I}} = \frac{2\sqrt{2\pi F(v)}}{3g^{5/2} z_0 C d_{eff}} D_{\max}^{5/2} \quad (1)$$

$$K_{II} = \mu K_I \quad (2)$$

where D_{max} is the maximum diameter of speckle-focus along the crack direction; z_0 is the distance from reference plane to object plane; C is stress optic constant; d_{eff} is effective thickness of the specimen, and for transparent materials, the effective thickness of the plate is the actual thickness of the plate; μ is coefficient of stress intensity factors; g is numerical factor of stress intensity; K_I and K_{II} is stress intensity factor of composite crack tip under dynamic loading. F(v) is correction factor caused by crack propagation velocity and in the practical significance of crack propagation velocity, its value is approximately equal to 1.

2.2. Determination of crack propagation velocity and acceleration

The crack tip position during the crack propagation can be precisely determined by the speckle-focus. Thus, the propagation crack length at each time instant is measured. In order to minimize data scattering in the evaluation of fracture parameters such as the crack velocity and acceleration, a data-fitting procedure proposed by Takahashi and Arakawa [9] is used to express the actual crack length L(t) as a ninth order polynomial of time t as shown in Eq. (3):

$$L(t) = \sum_{i=0}^{9} L_i t^i \quad (3)$$

where L(t) is the length of crack; the coefficient L_i is determined by the least-square method. Thus, the crack velocity v and acceleration a are determined from the first and second time derivative of the fitted curve L(t), respectively.

2.3. The relationship between dynamic energy release rate and the dynamic stress intensity factors

Energy release rate is the parameter to study the crack tip stress and strain field at energy viewpoint. It is the energy of per unit area released by elastic system during crack propagation. At the same time, it

reflect the crack driving force and shows the reduction of system potential energy when crack propagation per unit area. Freund [10] analyzed the relationship between dynamic energy release rate and the dynamic stress intensity factors:

$$G=\frac{1}{E}\left[A_I(\upsilon)K_I^2+A_{II}(\upsilon)K_{II}^2\right] \tag{4}$$

the formula above is expressed in case of plane stress. Where $A_I(\upsilon)$、$A_{II}(\upsilon)$ is function of crack propagation velocity.

as $\upsilon = 0$, $A_I(v)=A_{II}(v)=1$ (5)

as $\upsilon \neq 0$, $A_I(v)=\upsilon^2 a_d/\left((1-v)C_s^2 D\right)$, $A_{II}(v)=\upsilon^2 a_s/\left((1-v)C_s^2 D\right)$ (6)

$$D=4a_d a_s-\left(1+a_s^2\right)^2 \tag{7}$$

$$a_d=\sqrt{1-\upsilon^2/C_d^2}\ ,\ a_s=\sqrt{1-\upsilon^2/C_s^2} \tag{8}$$

And E is modulus of elasticity; C_d and C_s are expansion wave velocity and shear wave velocity, respectively; υ is crack propagation velocity. According to Eq. (4), dynamic energy release rate of the crack tip at each time can be obtained.

3. Experimental description

3.1. Test system

The main parts of dynamic caustics blast load test system are shown as follows: (1) Blast loading and protection; (2) Detonation method and detonation devices; (3) DDGS–II multi-spark high-speed photography experimental optical system; (4) Delay and control devices; (5) Light - electricity conversion system. The electronic control system to manage the spark discharge and the shooting time of caustics pictures are used. Pre-set time interval as needed. The time interval between two pictures is adjustable from 0 to 999μs. With this light - electricity system, clear pictures of dynamic caustics can be recorded

3.2. Specimen description

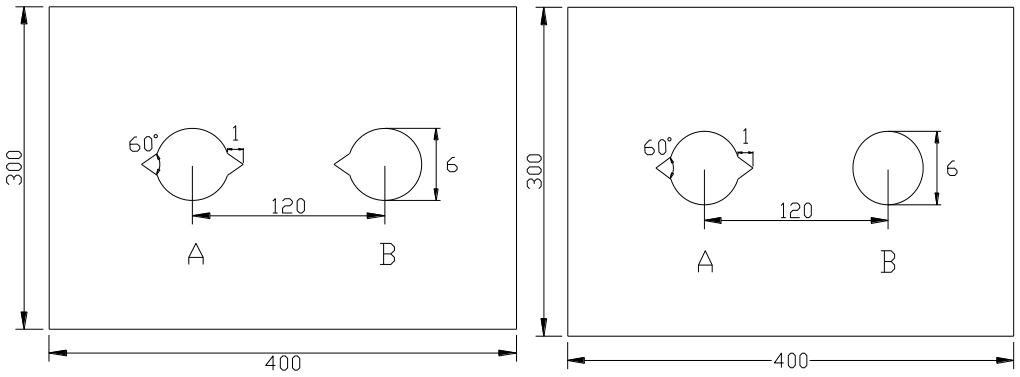

Fig.1. Grooving blast model

PMMA were used in this dynamic experiment. The specimen is of the thickness 5mm and dimensions

400×300mm^2. Two holes is in central of the specimen, spacing is 120mm, diameter is 6mm, grooving angle α is 60 °, grooving depth is 1mm. Designed two kinds of grooving modes: (a) and (b). (a): A-hole double grooving, B-hole single grooving. (b): A-hole double grooving, B-hole no grooving. Its geometrical form is shown in Fig. 1. Dynamic mechanical and optical properties of PMMA material are listed in Table 1. 140mg elemental lead azide explosives were loaded into each hole.

Table 1. Dynamic parameters of PMMA

$C_p/(m\bullet s^{-1})$	$C_s/(m\bullet s^{-1})$	$E_d/(N\bullet m^{-2})$	v_d	$\lvert C_t\rvert(m^2\bullet N^{-1})$
2320	1260	6.10×10^{9}	0.31	0.80×10^{-10}

4. Experimental results and analysis

4.1. Description of experimental phenomenon

Fig.2. Crack propagation of (a) and (b) under the condition of simultaneous initiation

Fig.2 shows the pictures of (a) and (b) after being broken. (a), due to the presence of grooving, crack AI, AO, BI firstly began to propagate along the grooving direction. Crack in grooving direction was longer than others. Perforated crack AI and BI did not directly encounter, but one was up and other was down, propagating to the other existing crack surface. 2-4 random cracks were also formed around the hole. Their direction and length were no statistical regulations. (b), B-hole is no grooving, BI which was generated randomly would be considered as perforated crack between the two holes.

4.2. Evolution of stress intensity factors

t=20μs t=40μs t=51μs t=85μs

Fig.3 shows the dynamic speckle-focus images of scheme (a). After simultaneous initiation of the two holes, P-wave and S-wave are produced. P-wave speed is 1.7 times as fast as S-wave. The two kinds of

blast wave separate in the dissemination process. P-wave propagates outward taking the hole as circle center, while the process of S-wave propagation is messier. Scattering and diffraction of stress wave at the crack tip, reflection at the specimen boundary, interference and superposition between stress waves, all these result in stress state of crack tip is very complex. t = 20μs, the two-hole explosion P-wave met each other, the maximum focus-speckle diameter of crack AI , BI was 8.6mm, 7.8mm, respectively. t = 51μs, stress wave met the other crack and interacted with it. By this time, crack AI, BI had extended 27.2mm, 26.8mm, respectively. Also a part of the strain energy was dissipated; coke speckle diameter was reduced to 7.0mm, 6.3mm, respectively. t ≈ 110μs, two perforated crack AI and BI met each other. The speckle-focus of the crack tip became distorted. Speckle-focus and crack propagation direction was no longer symmetrical. That was to say, crack tip stress field was complex with normal stress and shear stress together. Its size reflected the extent of the crack tip stress concentration. t=175μs, focus-speckle diameter was up to the second peak, 7.2mm, 6.7mm, respectively. This may be due to stress waves reflected from the boundary interacted with the crack tip, promoting crack propagation. Fig.4 shows the variations of complex stress intensity factors at crack tip. As can be seen from the curve, stress intensity factor decreased rapidly from the maximum, oscillated, and up to the second peak, then decreased until crack arrested. With crack propagation, K_I and K_{II} show oscillatory behavior. And during the process, K_I was almost grater than K_{II}. It can be concluded that during the process of stress wave interaction with crack tip, P-wave played a major role, and S-wave followed. This also provides an effective experimental basis is for the study of directional fracture controlled blasting.

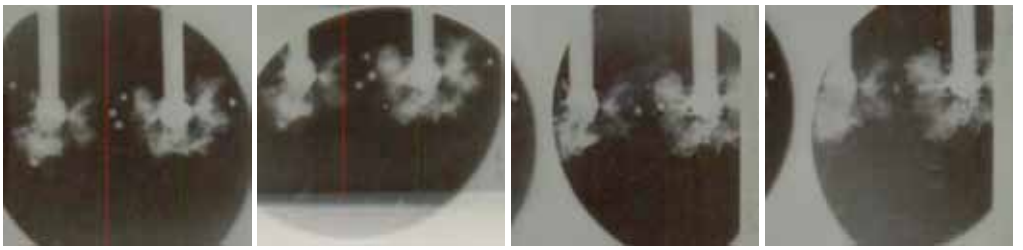

Fig.3. Dynamic speckle-focus images of scheme (a)

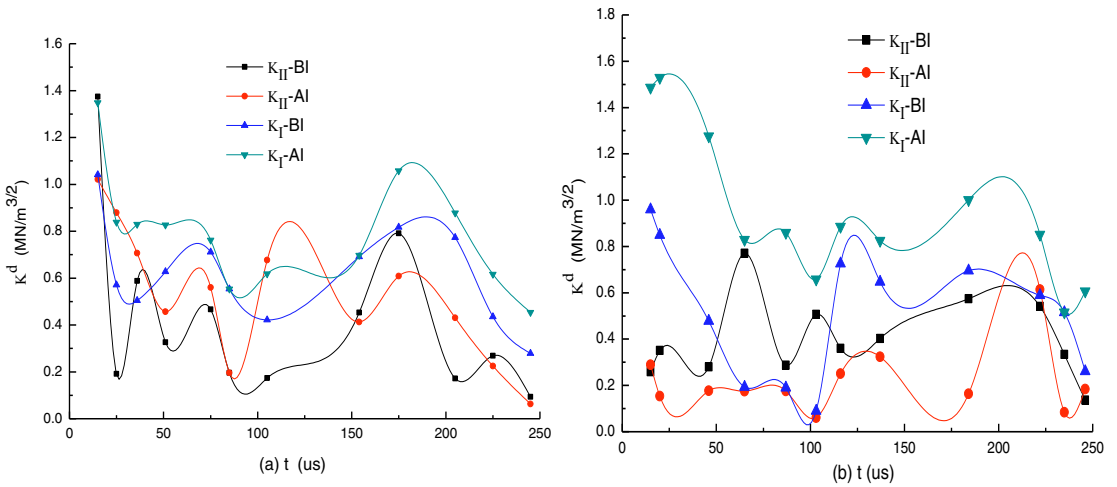

Fig.4. Variations of complex stress intensity factors at crack tip

4.3. Crack velocity and acceleration

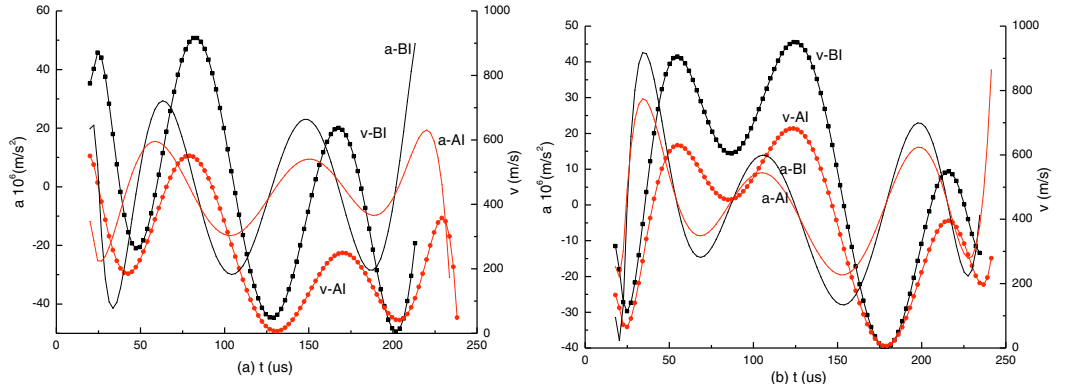

Fig.5. Variation of crack velocity and acceleration

Fig.5 shows the variation of crack velocity and acceleration. During the crack propagation process, the velocity v and acceleration a showed a type of fluctuation changes as wave. This further indicates that at the crack tip, scattering and diffraction of expansion wave produced by blast and tensile wave reflected back from the boundary have an impact on crack propagation. Velocity and acceleration were alternating up to their own peak. For a single crack, it was common that the acceleration firstly came to the peak, then the velocity came to the peak again, repeated many times. (a), t = 81μs, AI, maximum 550.8m/s; t = 81μs, BI maximum 915.6m/s. (b), t = 119μs, AI, maximum 675.3m/s; t = 123μs, BI maximum 920.1m/s. As the burst test is complex, uncontrollable, difficult to record the data, the time instant of maximum velocity is no statistical regulations. (a), t ≈ 130μs and (b), t ≈ 170μs, crack propagation velocity closed to zero. This might be due to interference of stress wave, inhibited crack propagation.

4.4. Dynamic energy release rate

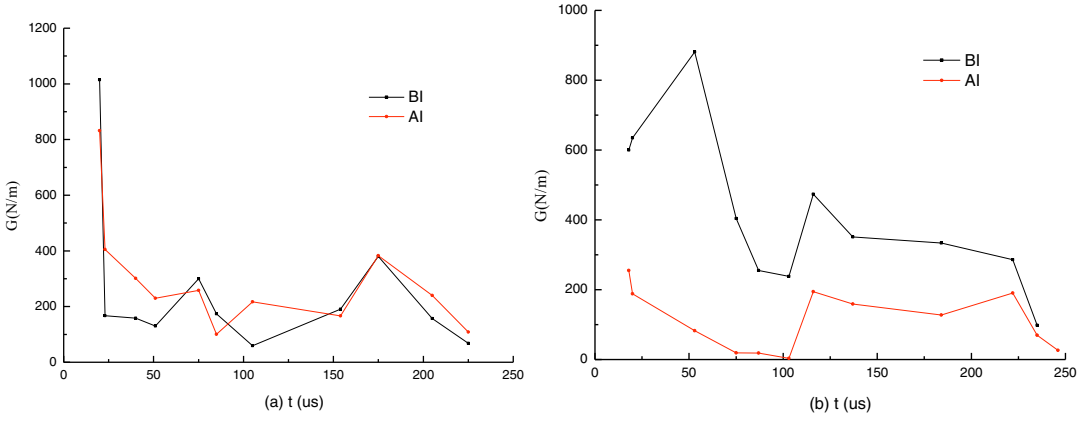

Fig.6. The dynamic energy release rate vs. time

(a), because of the limitations of experimental equipment, t = 20us, energy release rate at crack tip

began to be obtained. And at this time the energy release rate was maximal in all the data. AI, 831.6 N/m; BI, 1014.6 N/m, respectively. And decreased rapidly. According to this trend, it can be guessed that the energy release rate after split was smaller than before split. The difference between them reflected the dynamic energy release rate plays a driving role on crack propagation [11]. After explosion, the elastic strain stored at the crack tip suddenly released, which caused the energy release rate at crack tip suddenly dropping. $t \approx 75\mu s$, this trend began to converge, then oscillated. $t = 177\mu s$, up to the second peak. (b), $t = 53\mu s$, the energy release rate came to the peak as 880.8 N/m. After explosion but before crack propagation, potential energy of system was gradually transformed into elastic strain energy. Energy release rate increased with time increment. When it reached the required crack propagation energy per unit area G_I, the cracks began to propagate. The energy release rate decreased rapidly, then oscillated. $t = 120\mu s$, up to the second peak. This oscillation fully reflected the stress wave had an impact on crack propagation. Stress wave was carrying energy in propagation process. Stress wave interacted with the crack tip, changing the stress state of the specimen and the dynamics singular stress field of the crack tip, thus changing the status of crack propagation. Energy carried by stress wave was transferred to the crack, driving crack propagation. The variation energy release rate remained the same with the variation of the stress intensity factor. Dynamic energy release rate and the dynamic stress intensity factor had the same sense of dynamic fracture mechanics. The energy release rate drives crack propagation.

5. Conclusion

(1) Stress intensity factor decreased rapidly from the maximum, oscillated, and up to the second peak, then decreased until crack arrested. This change reflected the stress wave had an influence on crack propagation. K_I was almost grater than K_{II}. It can be concluded that during the process of stress wave interaction with crack tip, P-wave played a major role, and S-wave followed.

(2) The velocity and acceleration showed a type of fluctuation changes as wave. Scattering and diffraction of expansion wave produced by blast and tensile wave reflected back from the boundary have an impact on crack propagation. Acceleration firstly came to the peak, then the velocity came to the peak again, and repeated many times.

(3) The energy release rate decreased rapidly, oscillated, and then decreased. It remained the same with the variation of the stress intensity factor. Dynamic energy release rate and the dynamic stress intensity factor had the same sense of dynamic fracture mechanics. The energy release rate drives crack propagation.

Acknowledgements

This work was financially supported by the National Natural Science Foundation of China-Coal Joint Fund (51134025); National Natural Science Foundation of China (50874109)； Central University Basic Research Cost of Operation Special Fund (2011QL06).

References

[1] Li Qing. Experiment of fracture behaviors and control for crack propagation under blasting load [D]. Beijing: China university of mining and technology (Bei jing), 2009. (in Chinese)

[2] Zhang Zhicheng. Summary of the mechanism of directional fracture controlled blasting [J]. Mining Research and Development, 2000, 20(5): 40-42. (in Chinese)

[3] Huang Tao, Chen Pengwan, Zhang Guoxin, et al. Numerical simulation of two-hole blasting using numerical manifold method [J]. Explosion and Shock Waves, 2006, 26(5):434-440. (in Chinese)

[4] Kalthoff J F, Winkler S, Beinert J. Dynamic stress-intensity factors for arresting cracks in DCB specimens [J]. International Journal of Fracture, 1976, 12: 317-319.

[5] Theocaris P S. Dynamic propagation and arrest measurements by the method of caustics on overlapping kewparallel cracks [J]. International Journal of Solid and Structures, 1978 (14): 639-653.

[6] Yang Renshu. Caustics study of rock hole directional fracture controlled blasting mechanism. [D]. Beijing: China university of mining and technology (Beijing), 1997. (in Chinese)

[7] Yang Renshu, Yue Zhongwen, Xiao Tong she, et al. Dynamic caustics experiment on crack propagation of jointed medium fracture with controlled blasting [J]. Chinese Journal of Rock Mechanics and Engineering, 2008, 27 (2): 244-250. (in Chinese)

[8] Yang Renshu, Gui Laibao. Caustics method and its application [D]. Xuzhou: China university of mining and technology press, 1997. (in Chinese)

[9] K. Takahashi, K. Arakawa. Dependence of crack acceleration on the dynamic stress intensity factor in polymers [J], Experimental mechanics, 1987 (6): 195-217.

[10] Freund L B. Dynamic fracture mechanics [M]. Edinburgh: Cambridge University Press, 1990.

[11] Yao Xuefeng, Fang Jing. Analysis of caustics on dynamic energy release rate of running crack tip under impact load [J]. Explosion and Shock Waves, 1996, 16 (2): 111-116. (in Chinese) .